Journal of Applied Polymer Science

Synthesis and Characterization of Elastomeric Polyurethane and PU/Clay Nanocomposites Based on an Aliphatic Diisocyanate

Chinmoy Saha, Tapan K. Chaki, Nikhil K. Singha
Rubber Technology Centre, Indian Institute of Technology, Kharagpur 721302, India
Correspondence to: N. K. Singha (E-mail: nks8888@yahoo.com)

ABSTRACT: This investigation reports preparation of polyurethane and polyurethane/clay nanocomposites based on polyethylene glycol, isophorone diisocyanate (IPDI), an aliphatic diisocyanate and 1,4- Butanediol as chain extender by solution polymerization. In this case PU/clay nanocomposites were prepared via *ex-situ* method using 1, 3, and 5 wt % of Cloisite 30B. Thermogravimetric analysis showed that the maximum decomposition temperature (T_{max}) of the PU/clay nanocomposite is much higher than the pristine PU. The tensile properties improved upon increasing the organoclay (Cloisite 30B) content upto 3 wt %, and then decreased to some extent upon further increasing the nanoparticle loading to 5 wt %. Optical properties of the nanocomposites were studied by UV-vis spectrophotometer. X-ray diffraction (XRD) and transmission electron microscopy (TEM) were used to study the morphology of the nanocomposites. It was observed that with the incorporation of 3 wt % nanoclay the crystallinity in PU nanocomposite increases, then diminishes with further loading. © 2013 Wiley Periodicals, Inc. J. Appl. Polym. Sci. 130: 3328–3334, 2013

KEYWORDS: polyurethane, isophorone diisocyanate (IPDI), nanocomposite, nanoclay, XRD, TEM

Received 14 December 2013; accepted 10 May 2013; Published online 17 June 2013
DOI: 10.1002/app.39534

INTRODUCTION

Polyurethane (PU) is a segmented polymer with wide range of physical and chemical properties. It has hard and soft segment. The hard segment is formed by the reaction of diisocyanate and chain extender. The two phase morphology of the polyurethane occurs due to incompatibility between hard and soft segment. Morphology of the polyurethane is the determining factor of its thermal and mechanical property.[1–4] The soft segment generally consists of polyester and polyether diol, which influences the elastic nature of elastomer. Now-a-days different types of monomers with wide range of properties are commercially available, which can be used to prepare polyurethane with unique combination of properties. The isocyanate building blocks in segmented polyurethane elastomers can be either aromatic or aliphatic. The aromatic isocyanates are more reactive than aliphatic isocyanates, which can only be utilized if their reactivity matches with the specific polymer reaction and special properties desired in the final product. For example, polyurethane coatings made from aliphatic isocyanates are light stable,[5] while coatings made from an aromatic isocyanate undergo photodegradation. Aliphatic isocyanates, like hydrogenated methylene diphenyl diisocyanate (HMDI) and isophorone diisocyanate (IPDI) are preferred for the production of transparent polyurethane elastomers. Transparency arises, because of the presence of geometric isomer in these isocyanates. Typically IPDI is a mixture of 28% trans and 72% cis isomer.

Polyurethanes are widely used to prepare coatings, adhesives, and foams. However, polyurethanes have some disadvantages, such as poor thermal stability and poor gas-barrier properties. These disadvantages are overcome by introducing inorganic fillers, especially nanoclay based on Montmorillonite (MMT). MMT consists of octahedral sheet of alumina, sandwiched between two external silica tetrahedrons and is widely used to prepare polymer composite. Due to the presence of sodium cations in the interlayer spaces (galleries), MMT is hydrophilic in nature and has poor compatibility towards organic polymer. Therefore, alkali metal cations are usually exchanged with hydrophobic organic cations to improve the compatibility of MMT with organic polymers.[6–8]

After the pioneering work of Toyota's group in Nylon-clay nanocomposites,[9] there has been plethora of reports on polymer/clay nanocomposites based on different polymers, such as, polycaprolactone/organoclay,[10–12] polystyrene/ organoclay,[13,14] epoxy/organoclay,[15–18] polyimide/organoclay,[19,20] fluoroelastomers/organoclay,[21–24] styrene butadiene rubber/organoclay,[25] ethylene propylene diene rubber/acrylonitrile butadiene rubber/organoclay[26] and poly(methyl methacrylate)/ organoclay.[27–29] There have been also extensively studies on PU/MMT nanocomposites[30–34] to enhance the properties of PUs for wide range of application. However, to the best of

Additional Supporting Information may be found in the online version of this article.

Table I. Proportion of Various Ingredients Used in the Preparation of Polyurethane and Its Nanocomposite

Sample	Clay content (wt%)	IPDI/polyol/BD
PU-PG-C30B-0	0	2/1/1
PU-PG-C30B-1	1	2/1/1
PU-PG-C30B-3	3	2/1/1
PU-PG-C30B-5	5	2/1/1

our knowledge there is no detailed report on PU/clay nanocomposite based on IPDI. Being an aliphatic diisocyanate IPDI has excellent UV resistance, thermal resistance property and also has good optical property.

This investigation reports the preparation and characterization of PU based on polyethylene glycol [PEG], isophorone diisocyanate (IPDI), an aliphatic diisocyanate and 1,4- Butanediol (BD) as chain extender and its nanocomposite based on organically modified nanoclay (Cloisite 30B) via *ex-situ* technique and evaluation of their morphology, mechanical and thermal properties.

EXPERIMENTAL

Materials

Polyethylene glycol (PEG), (molecular weight 300), was procured from Sigma-Aldrich Chemicals, Bangalore, India. Isophorone diisocyanate (IPDI) was purchased from Sigma-Aldrich Chemicals, Bangalore, India. The clay, Cloisite 30B was purchased from Southern Clay Products, Gonzales, TX. It had 90 meq of quaternary ammonium ions/100 g of clay. The quaternary ammonium ion has a structure of $N^{+}(CH_2CH_2OH)_2(CH_3)T$, with T representing an alkyl group of approximately 65% $C_{18}H_{37}$, 30% $C_{16}H_{33}$, and 5% $C_{14}H_{29}$. Dibutyltin dilaurate (DBTDL) and 1,4-butanediol (BD) were procured from Aldrich Chemicals, Bangalore, India. Tetrahydrofuran (THF) and diethylether were purchased from Merck Specialities Private Limited, Mumbai, India.

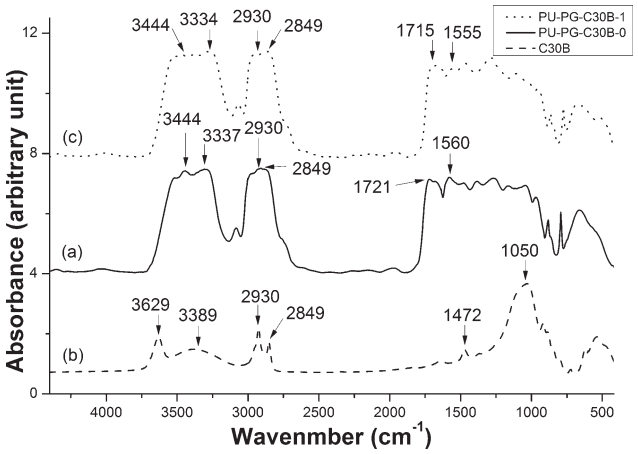

Figure 1. FT-IR spectra of (a) pristine polyurethane prepared from IPDI, PEG and BD, (b) clay (Cloisite 30B), and (c) polyurethane-clay nanocomposite.

Synthesis of the PU

Table I represents proportion of various ingredients used in the synthesis of polyurethane. The ratio of –NCO and –OH functional groups was maintained at 1:1. PEG and 1,4-butanediol were weighed in a three neck round bottom flask and test tube respectively. Both materials were dried in a vacuum oven at 60°C for 24

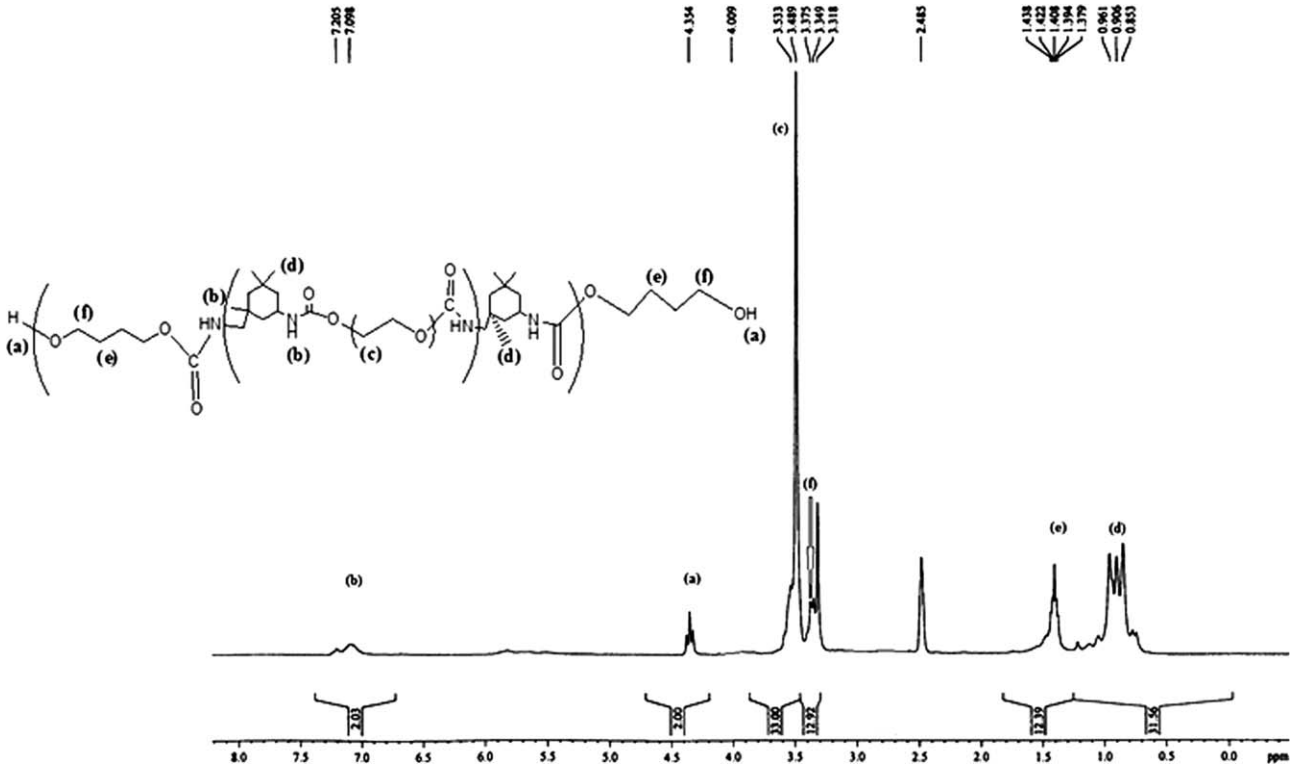

Figure 2. NMR spectra of the polyurethane prepared from IPDI, PEG, and BD.

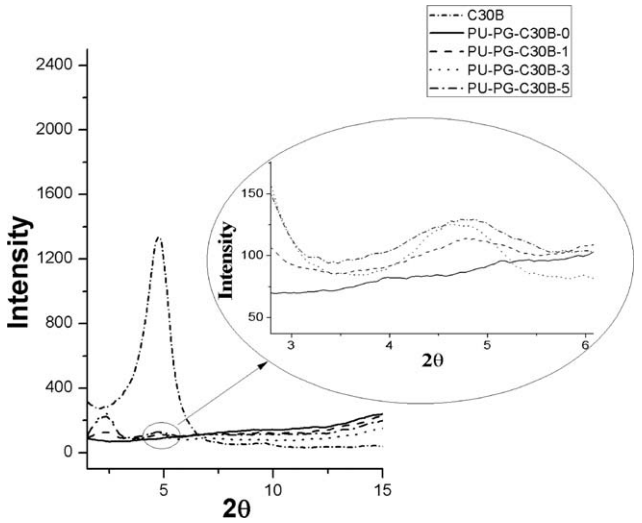

Figure 3. WAXD patterens at lower angular range of PU/Cloisite 30B nanocomposites.

h. Dry THF (5 mL) was added to PEG and placed it in an oil bath and heated to 70°C with stirring at 850 rpm. Nitrogen gas was purged through the round bottom flask for half an hour. IPDI and the catalyst, DBTDL were separately dissolved in dry THF and were added to the reaction mixture. After complete addition of IPDI the reaction was carried out for two and half hours. The prepolymer formed was precipitated in diethylether. The precipitated prepolymer again dissolved in dry THF and BD dissolved in dry THF was added to it. The reaction was carried out at 70°C with stirring at 850 rpm for one and half hour. The polymer solution was directly casted into teflon petridish, dried at ambient temperature for 12 h and then in vacuum oven at 60°C for 3 days.

Preperation of PU/Clay Nanocomposite

First the clay was dried in vacuum oven for 6 h. The polymer was dissolved in THF by stirring. The clay was sonicated in THF for 1 h and then was completely transferred to the polymer solution. The polymer–clay solution was stirred for another 15 min and was sonicated for another half an hour. Then the solution was poured into a teflon petridish and was kept at ambient temperature for 12 h to slowly evaporate the solvent. Finally the cast films were dried in a vacuum oven at 60°C for 3 days.

Characterization

FT-IR studies were carried out on thin film samples using a Perkin-Elmer FT-IR spectrophotometer (model spectrum RX I), within a range of 400–4400 cm^{-1} using a resolution of 4 cm^{-1}. An average of 16 scans was reported for each sample.

NMR spectroscopy of the compounds was carried out using Bruker AC 200 MHz NMR Spectrometer. DMSO-D_6 was used as solvent for all the studies. An average of 16 scans was reported for each sample.

The XRD patterns of the samples were recorded in a Philips X-ray diffractometer (model PW-1710) at crystal monochromated Cu Kα radiation in the angular range of 2–15° (2θ) at 40 kV operating voltage and 20 mA current. Each sample was tested for three times.

The samples for TEM analysis were prepared by ultracryomicrotomy with a Leica Ultracut UCT (Leica Mikrosystems GmbH, Vienna, Austria). Freshly sharpened glass knives with cutting edges of 45° were used to obtain cryosections of 50–70 nm thickness. [As the samples are elastomeric in nature. The sample and glass knife temperatures during ultracryomicrotomy were kept constant at −50°C and −60°C, respectively. These temperatures were well below the glass transition temperatures (T_g's) of PUs]. The cryosections were collected individually in a sucrose solution and was directly supported on a copper grid of 300 meshes in size. Microscopy was performed with a JEOL JEM 2010 TEM instrument (Japan), operating at an accelerating voltage of 120 kV.

Tensile specimens were punched out from the cast sheets using ASTM Die-C. The tests were carried out as per the ASTM D 412-98 method in a Universal Testing Machine (Zwick 1445) at a cross-head speed of 100 mm/min at 25°C. All the samples were tested for three times and the results were reported as the average of triplicates.

Differential scanning calorimetry (DSC) analysis was carried out by using TA Instrument (DSC Q100 V8.1 Build 251) under nitrogen atmosphere from −40°C to 40°C at a heating rate of 20°C/min. The glass transition temperature (T_g) was determined from the inflexion point of the second heating cycle.

TGA was carried out in the TA Instruments (model Q50) under nitrogen atmosphere. In this case about 5 mg sample was heated at 30°C to 600°C, at the heating rate of 20°C/min. Each sample was tested for three times and the results were reported as the average of triplicates.

UV-vis transparency was performed on a Shimadzu UV-3600 UV-vis NIR spectrophotometer over the wavelength range of 200–700 nm. Thin films of 0.2 mm were measured for optical transparency with the percent transmittance at 550 nm (the solar maximum) reported.

RESULTS AND DISCUSSION

FT-IR Characterization

Polyurethane (PU) was prepared by using IPDI as aliphatic diisocyanate and polyethylene glycol (PEG) as polyether polyol and 1,4-

Table II. WAXD Analysis and Tensile Properties of Synthesized Polyurethane and Its Nanocomposite

Sample	Wt % of clay	2θ	Width of tactoids (Å)	Tensile strength (MPa)	Elongation at break (%)
Cloisite 30B		4.74°	67.3 ± 0.0005		
PU-PG-C30B-0	0			10.88 ± 0.21	583 ± 5
PU-PG-C30B-1	1	4.76°	93.7 ± 0.0007	11.78 ± 0.35	524 ± 8
PU-PG-C30B-3	3	4.58°	92.7 ± 0.0007	14.13 ± 0.30	550 ± 7
PU-PG-C30B-5	5	4.71°	79.6 ± 0.0006	11.02 ± 0.24	546 ± 8

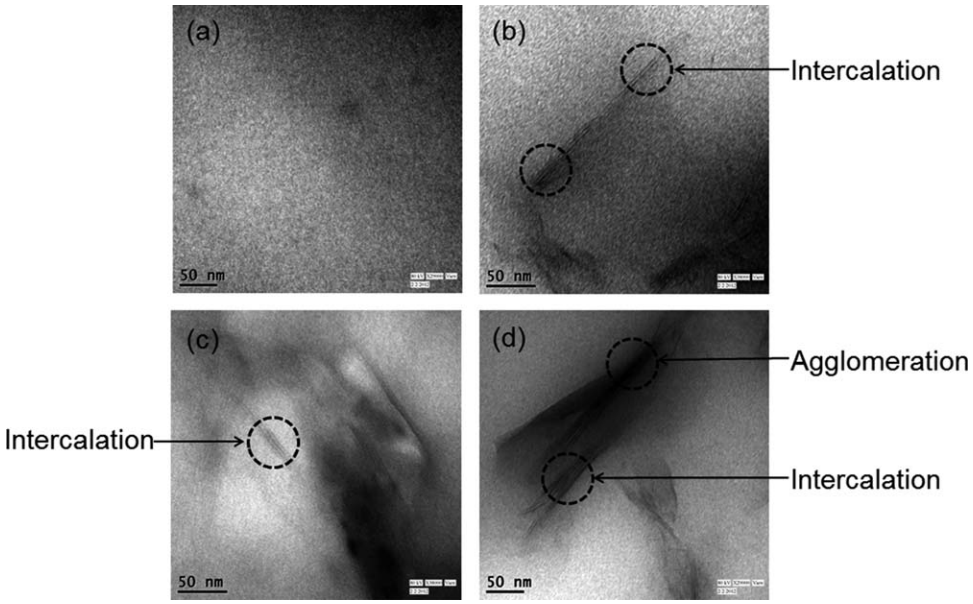

Figure 4. TEM photomicrograph of (a) virgin polymer and composites with (b) 1%, (c) 3% and (d) 5% clay (Cloisite 30B) at 29 KX magnification.

butanediol (BD) as a chain extender. Figure 1 shows the FT-IR spectra of PU [Figure 1(a)], clay (Cloisite 30B) [Figure 1(b)] and PU/clay nanocomposite [Figure 1(c)]. The FT-IR spectrum [Figure 1(a)] of synthesized PU shows -NH absorption peaks at 3337 cm^{-1} and 1560 cm^{-1} which are due to the hydrogen bonded -NH stretching and –NH bending in the urethane linkages respectively, while >C═O stretching bands appear at 1721 cm^{-1} and 1704 cm^{-1} which are due to free and hydrogen bonded carbonyls respectively.[35] The peak at 3444 cm^{-1} may be due to presence of terminal hydroxyl group. The strong absorption band at 1100 cm^{-1} appears due to polyether linkages present in polymer chain.[36] The absence of peak at 2260 cm^{-1} indicates the completion of reaction between the hydroxyl and isocyanate group.

The FT-IR spectrum [Figure 1(b)] of the clay (Cloisite 30B) shows a broad peak at 1050 cm^{-1}, which corresponds to the Si—O stretching of in the montmorillonite clay. The peaks at 3629 cm^{-1} and 3389 cm^{-1} correspond to stretching vibrations of structural —OH group and OH stretching of loosely bound water

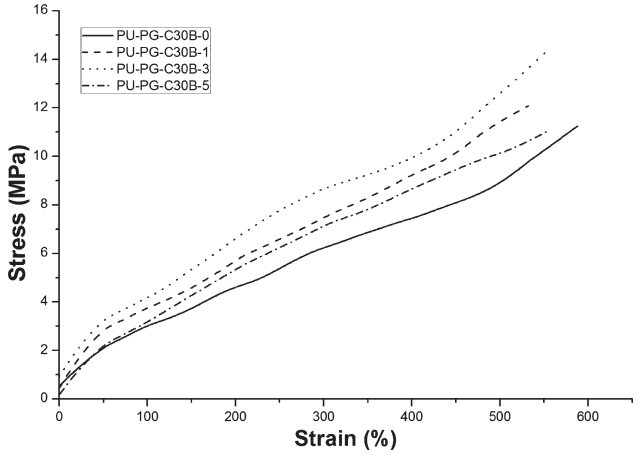

Figure 5. Stress/Strain curve of PU/Clay (Cloisite 30B) nanocomposite.

respectively. Organic modifier in the clay shows peaks at 2930 and 2849 cm^{-1} due to aliphatic C—H stretching and at 1472 cm^{-1} for C—H bending.[37] Figure 1(c) shows the FT-IR spectrum of PU/clay nanocomposite. Comparison of this spectrum with the same of the pristine PU (Figure 1) shows that the free >C═O stretching band shifted from 1721 cm^{-1} to 1715 cm^{-1} and N—H bending vibration peak shifted from 1560 cm^{-1} to 1555 cm^{-1}. This confirms the interaction of clay with PU.[38]

NMR Studies

Figure 2 shows the ^{1}H-NMR spectra and chemical structure of the synthesized PU. The presence of resonances at 7.02 (b) confirms the presence of proton in urethane linkage.[39] The occurrence of a triplet at 4.35(a) confirms the presence of terminal hydroxyl proton. The presence of resonance at 3.5(c) is due to protons of polyethylene glycol. The resonances at 3.3(f) and 1.4(e) appear due to outer and rear protons of BD, respectively. The resonances at 0.9(d) appear due to the protons of IPDI.[40]

XRD Studies

The WAXD pattern of PU/clay nanocomposite is shown in the Figure 3. The organoclay (Cloisite 30B) was used for nanocomposite preparation, because of its good delaminating and dispersing behavior in PU matrix.

Figure 3 shows the WAXD patterns of PU, Cloisite 30B and their composite. Cloisite 30B shows an intense peak at $2\theta = 4.74°$ for d_{001} plane with d-spacing of 18.6 Å. In PU/Cloisite 30B nanocomposites, the WAXD peak at $2\theta = 4.74°$ almost disappeared, but a relatively strong new peak appears at $2\theta = 2.4°$.[41] This indicates significant intercalation as well as formation of small tactoids below 100 nm size in the hybrid material. Schere equation was used to determine the size of the tactoids.[42] The details of the XRD analysis with standard deviation are shown in Table II.

This indicates that the 2θ value decreases up to 3 wt % of clay loading and then increases. It can also be observed that the size

Applied Polymer SCIENCE

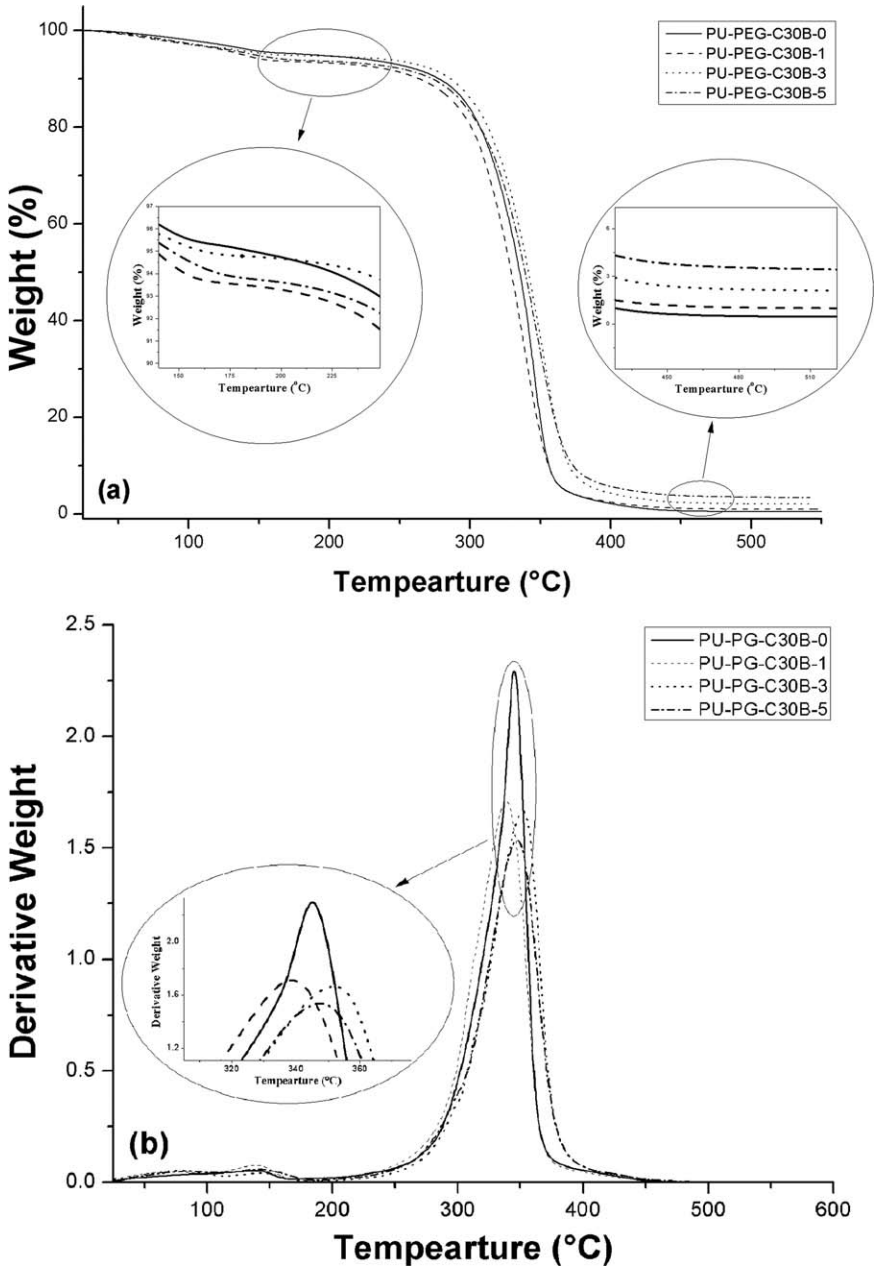

Figure 6. (a) TGA and (b) DTG curves of PU/Clay (Cloisite 30B) nanocomposite.

of the tactoids increases with the formation of nanocomposites, but at 5 wt % of clay loading the size of the tactoids decreased. The changes observed in the XRD data can be explained by the fact that the polymer enters into the clay galleries pushing the platelets apart, which in turn helps in the increase in the size of the tactoids. As more polymers enter into the galleries, the platelets lose their ordered structure. This results in the broadening of XRD peak. However, with 5 wt % of clay loading the size of

Table III. Thermal Properties of Synthesized Polyurethane and Its Nanocomposite

Sample	Composites with clay loading (%)	Glass transision temperature (T_g) (°C)	T_{onset} (°C) [10 wt% decomposition]	T_{max} (°C)	Final degradation temperature (°C)	Residue (wt %)
PU-PG-C30B-0	0	−6.5	278.0 ± 1.2	344.7 ± 1.0	366.8 ± 1.0	0.49 ± 0.01
PU-PG-C30B-1	1	−4.4	263.0 ± 1.0	339.5 ± 1.2	367.0 ± 1.0	0.97 ± 0.02
PU-PG-C30B-3	3	−1.8	285.7 ± 1.5	352.0 ± 1.0	391.5 ± 1.5	2.10 ± 0.01
PU-PG-C30B-5	5	−0.8	273.8 ± 1.0	347.9 ± 1.0	411.3 ± 1.5	3.39 ± 0.01

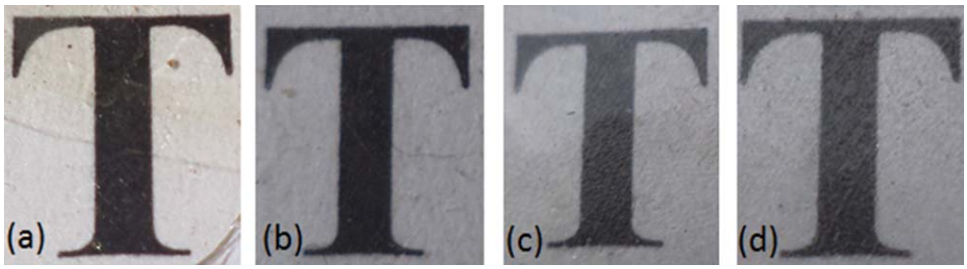

Figure 7. Visibility through PU/clay composite films: (a) Pristine polyurethane, (b) composite with 1% clay loading, (c) composite with 3% clay loading and (d) composite with 5% clay loading.

the tactoids decreased. This may be mainly attributed to the agglomeration of nanoclay above its critical content.

Morphological Analysis

TEM images of virgin polymer and with different loading of clay (1, 3, and 5 wt % of PU/Clay nanocomposite) are shown in Figure 4(a–d). Figure 4(c) shows the abundance of well-dispersed nanocomposite throughout the entire PU matrix without any agglomeration. There are agglomerations in 5% clay-loaded nanocomposite [Figure 4(d)]. It is seen that dispersion is good in 3 % clay loading. Figure 4(c), shows that the tactoids are arranged parallelly, which in turn increase the crystallinity of the sample. This is reflected in mechanical and thermal properties of the composites.

Tensile Properties

Figure 5 shows that the tensile property of PU and its composites. It indicates that tensile strength increases with increase in clay loading and attains the maxima at 3 wt % of nanoclay loading.[30] This is due to better dispersion of nanoclay, which results in intercalation morphology. This was corroborated by WAXD and TEM analysis, as explained earlier.

Thermal Analysis

Thermal stability of the PU and PU/clay nanocomposites were analyzed by TGA and DTG analysis. Figure 6 shows the comparative TGA and DTG curves of PU and PU/clay composites.

The onset temperatures (at 10 wt % decomposition) and T_{max} of different samples are reported in Table III. It shows that the onset degradation temperature of the polymer/clay composite is lower than that of the virgin PU. This is due to the early loss of quaternary ammonium ions in the clay which undergo the Hoffman elimination during the onset degradation.[42] But after the preliminary degradation the char acts as a barrier. So the T_{max} increases with increase in nanoclays. The improvement in the maximum degradation temperature is due to homogenous dispersion of the clay nanoplatelets in the polyurethane matrix.

The glass transition temperatures (T_g) of PU and PU/clay composites were determined from DSC analysis. The T_g values of different samples have been summarized in the Table III. It shows that T_g of PU composite increases on addition of nanoclay. This is due to presence of nanoclay, which restricts the segmental mobility of the polymer chains.

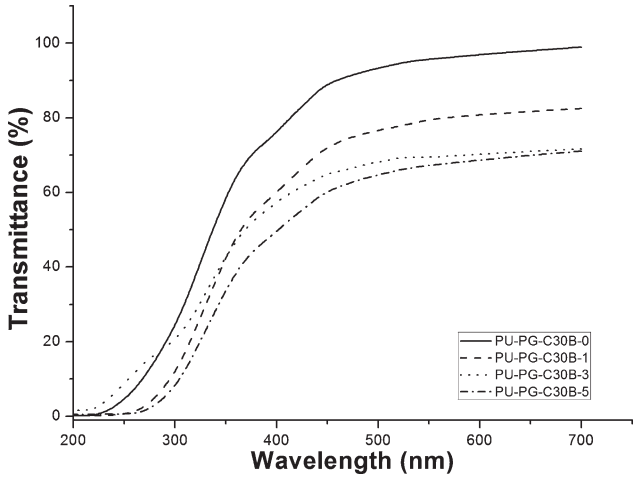

Figure 8. UV-vis transmittance of polyurethane/clay (Cloisite 30B) nanocomposite.

UV-Vis Studies

PU prepared using aromatic diisocyanates are generally opaque in nature.[43] The PU prepared in this investigation using aliphatic diisocyanate is highly transparent. Figure 7 shows the transparency of the pristine PU film and PU/Cloisite 30B nanocomposite film. It indicates PU film as well as its composite films have good transparency. UV-visible transmittance analysis (Figure 8) shows that pristine PU shows very high transmittance of 96%, but on clay loading the transparency decreases. However, the PU/clay nanocomposites have sufficient transparency, so that they can be used as transparent coatings.[44]

CONCLUSIONS

In this work, we have demonstrated the preparation of transparent polyurethane and polyurethane clay nanocomposite based on IPDI as an aliphatic diisocyanate. The structure of the polyurethane was characterized by ^{1}H-NMR and FT-IR analysis. The dispersion of clay and morphology were analyzed by TEM, XRD analysis. This indicates that nanoclays were intercalated within the PU matrix. There were improvements in the tensile properties and thermal properties on addition of nanoclay in the PU matrix. UV-vis analysis indicates that this PU based on aliphatic diisocyanate and its nanocomposites can be used as potential polymeric material for transparent coatings.

ACKNOWLEDGMENT

Financial support of Council of Scientific and Industrial Research (CSIR), New Delhi, India, for this work is gratefully acknowledged.

REFERENCES

1. Garrett, J. T.; Runt, J.; Lin, J. S. *Macromolecules* **2000**, *33*, 6353.
2. Miller, J. A.; Lin, S. B.; Hwang, K. K. S.; Wu, K. S.; Gibson, P. E.; Cooper, S. L. *Macromolecules* **1985**, *18*, 32.
3. Wang, C. B.; Cooper, S. L. *Macromolecules* **1983**, *16*, 775.
4. Mishra, A. K.; Mushtaq, S.; Nando, G. B.; Chattopadhyay, S. *Rheologica Acta* **2010**, *49*, 865.
5. Frisch, K. C. *Rubber Chem. Technol.* **1972**, *45*, 1442.
6. Liu, X. W.; Hu, M.; Hu, Y. H. *J. Cent. South. Univ. T.* **2008**, *15*, 193.
7. Bhattacharyya, K.; Gupta, S. *Adv. Colloid Interface Sci.* **2008**, *140*, 114.
8. Diamond, S.; Kinter, E. B. in Tenth National Conference on Clays and Clay Minerals, Austin, Texas, **1961**, p 163.
9. Giannelis, E. P. *Adv. Mater.* **1996**, *8*, 29.
10. Chavarria, F.; Nairn, K.; White, P.; Hill, A. J.; Hunter, D. L.; Paul, D. R. *J. Appl. Polym. Sci.* **2007**, *105*, 2910.
11. Sabet, S. S.; Katbab, A. A. *J. Appl. Polym. Sci.* **2009**, *111*, 1954.
12. Di, Y.; Iannace, S.; Di Maio, E.; Nicolais, L. *J. Polym. Sci., Part B: Polym. Phys.* **2003**, *41*, 670.
13. Chigwada, G.; Wang, D.; Jiang, D. D.; Wilkie, C. A. *Polym. Degrad. Stab.* **2006**, *91*, 755.
14. Ghosh, A. K.; Woo, E. M. *Polym. J.* **2004**, *45*, 4749.
15. Xue, S.; Pinnavaia, T. J. *Microporous Mesoporous Mater.* **2008**, *107*, 134.
16. Solar, L.; Nohales, A.; Muñoz-Espí, R.; López, D.; Gómez, C. M. *J. Polym. Sci., Part B: Polym. Phys.* **2008**, *46*, 1837.
17. Ngo, T. D.; Ton-That, M. T.; Hoa, S. V.; Cole, K. C. *J. Appl. Polym. Sci.* **2008**, *107*, 1154.
18. Langat, J.; Bellayer, S.; Hudrlik, P.; Hudrlik, A.; Maupin, P. H.; Gilman, J. W.; Raghavan, D. *Polym. J.* **2006**, *47*, 6698.
19. Campbell, S. *High Perform. Polym.* **2006**, *18*, 71.
20. Tyan, H.-L.; Leu, C.-M.; Wei, K.-H. *Chem. Mater.* **2001**, *13*, 222.
21. Lakshminarayanan, S.; Gelves, G. A.; Sundararaj, U. *J. Appl. Polym. Sci.* **2011**, *124*, 5056.
22. Gao, J.; Gu, Z.; Song, G.; Li, P.; Liu, W. *Appl. Clay Sci.* **2008**, *42*, 272.
23. Valsecchi, R.; Viganò, M.; Levi, M.; Turri, S. *J. Appl. Polym. Sci.* **2006**, *102*, 4484.
24. Maiti, M.; Bhowmick, A. K. *J. Polym. Sci., Part B: Polym. Phys.* **2006**, *44*, 162.
25. Sadhu, S.; Bhowmick, A. K. *J. Appl. Polym. Sci.* **2004**, *92*, 698.
26. Ersali, M.; Fazeli, N.; Naderi, G. *Int. Polym. Proc.* **2012**, *XXVII*, 187.
27. Cui, L.; Tarte, N. H.; Woo, S. I. *J. Appl. Polym. Sci.* **2008**, *110*, 784.
28. Cui, L.; Tarte, N. H.; Woo, S. I. *Macromolecules* **2008**, *41*, 4268.
29. Chang, C.-C.; Hou, S.-S. *Eur. Polym. J.* **2008**, *44*, 1337.
30. Dan, C. H.; Lee, M. H.; Kim, Y. D.; Min, B. H.; Kim, J. H. *Polym. J.* **2006**, *47*, 6718.
31. Khudyakov, I. V.; Zopf, D. R.; Turro, N. J. *Des. Monomers. Polym.* **2009**, *12*, 279.
32. Pattanayak, A.; Jana, S. C. *Polym. J.* **2005**, *46*, 3394.
33. Pattanayak, A.; Jana, S. C. *Polym. Eng. Sci.* **2005**, *45*, 1532.
34. Thirumal, M.; Khastgir, D.; Singha, N. K.; Manjunath, B. S.; Naik, Y. P. *J. Macromol. Sci. Part A Pure Appl. Chem.* **2009**, *46*, 704.
35. Bouchemal, K.; Briançon, S.; Perrier, E.; Fessi, H.; Bonnet, I.; Zydowicz, N. *Int. J. Pharm.* **2004**, *269*, 89.
36. Keleş, E.; Hazer, B. *J. Polym. Environ.* **2009**, *17*, 153.
37. Nayak, P.; Singh, B. K. *Bull. Mater. Sci.* **2007**, *30*, 235.
38. Deka, H.; Karak, N. *Nanoscale Res. Lett.* **2009**, *4*, 758.
39. Sumi, M.; Chokki, Y.; Nakai, Y.; Nakabayashi, M.; Kanzawa, T. *Die. Makromol. Chem.* **1964**, *78*, 146.
40. Prabhakar, A.; Chattopadhyay, D. K.; Jagadeesh, B.; Raju, K. V. S. N. *J. Polym. Sci., Part A: Polym. Chem.* **2005**, *43*, 1196.
41. Dai, X.; Xu, J.; Guo, X.; Lu, Y.; Shen, D.; Zhao, N.; Luo, X.; Zhang, X. *Macromolecules* **2004**, *37*, 5615.
42. Beall, G. W.; Powell, C. E. In Fundamentals of Polymer-Clay Nanocomposites; Cambridge University Press, **2011**, Chapter 2, p 24.
43. Lakshminarayanan, S.; Gelves, G. A.; Sundararaj, U. *J. Appl. Polym. Sci.* **2012**, *124*, 5056.
44. Kim, B. K.; Seo, J. W.; Jeong, H. M. *Eur. Polym. J.* **2003**, *39*, 85.